Transportation Research Part C 123 (2021) 102968

Contents lists available at ScienceDirect

Transportation Research Part C

journal homepage: www.elsevier.com/locate/trc

Robust flight planning impact assessment considering convective phenomena

Javier García-Heras [a], Manuel Soler [a], Daniel González-Arribas [a], Kurt Eschbacher [b], Carl-Herbert Rokitansky [b], Daniel Sacher [c], Ulrike Gelhardt [c], Jürgen Lang [c], Thomas Hauf [d], Juan Simarro [e], Alfonso Valenzuela [f], Antonio Franco [f], Damián Rivas [f]

[a] Universidad Carlos III de Madrid, Leganés 28911, Spain
[b] Paris-Lodron Universität Salzburg, Salzburg 5020, Austria
[c] MeteoSolutions GmbH. Wilhelminenstraße 2, D-64283 Darmstadt, Germany
[d] Leibniz University of Hannover, Germany
[e] Agencia Estatal de Meteorología (AEMET), Spain
[f] Universidad de Sevilla, 41092 Sevilla, Spain

ARTICLE INFO

Keywords:
Robust flight-planning
Convective weather
Simulation

ABSTRACT

Thunderstorms are one of the leading causes of Air Traffic Management delays. In this paper, we assess how incorporating convective information into flight planning algorithms can lead to reductions in reroutings due to storm encounters during the execution of the flight. We use robust open-loop optimal control methodology at the flight planning level and incorporate meteorological uncertainties based on Ensemble Prediction System forecasts. Convective risk areas can be derived from the latter to be included in the objective function. At the execution level, the planned trajectories are included in an air traffic simulator (NAVSIM) under observed weather (wind and storms). In this simulation process, track modifications might be triggered in case of encountering an observed thunderstorm. A tool termed DIVMET based on pathfinding algorithms has been integrated into NAVSIM is considered to that end. Results show that planning robust trajectories (avoiding thus convective areas) reduces the number of storms encounters and increases predictability. This increase in predictability is at a cost in terms of fuel and time, also quantified.

1. Introduction

In the Air Traffic Management (ATM) system, convective weather conditions, especially thunderstorms, represent a significant source of disruption, delays, and safety hazards. Flying through a thunderstorm poses several hazards, such as heavy turbulence, windshear, downbursts, icing, lightning, and hail. Thus, aircraft should stay aware of these threats, tactically changing their flight plans when thunderstorm activity is encountered. When aggregated over multiple flights, these deviations amount to substantial air traffic disruptions and capacity reductions that the ATM system has to deal with, often by holding, delaying or canceling other flights. As an illustration, weather phenomena in 2018 caused 25.4% of ATFM's en-route delay (54.9% for Airport ATFM delay) adding up to around 4.8 million minutes of delay (en-route & airport) in the airspace of the European Civil Aviation Conference (ECAC) airspaces,

E-mail address: javier.garcia-heras@uc3m.es (J. García-Heras).

https://doi.org/10.1016/j.trc.2021.102968
Received 8 June 2020; Received in revised form 14 December 2020; Accepted 5 January 2021
Available online 5 February 2021

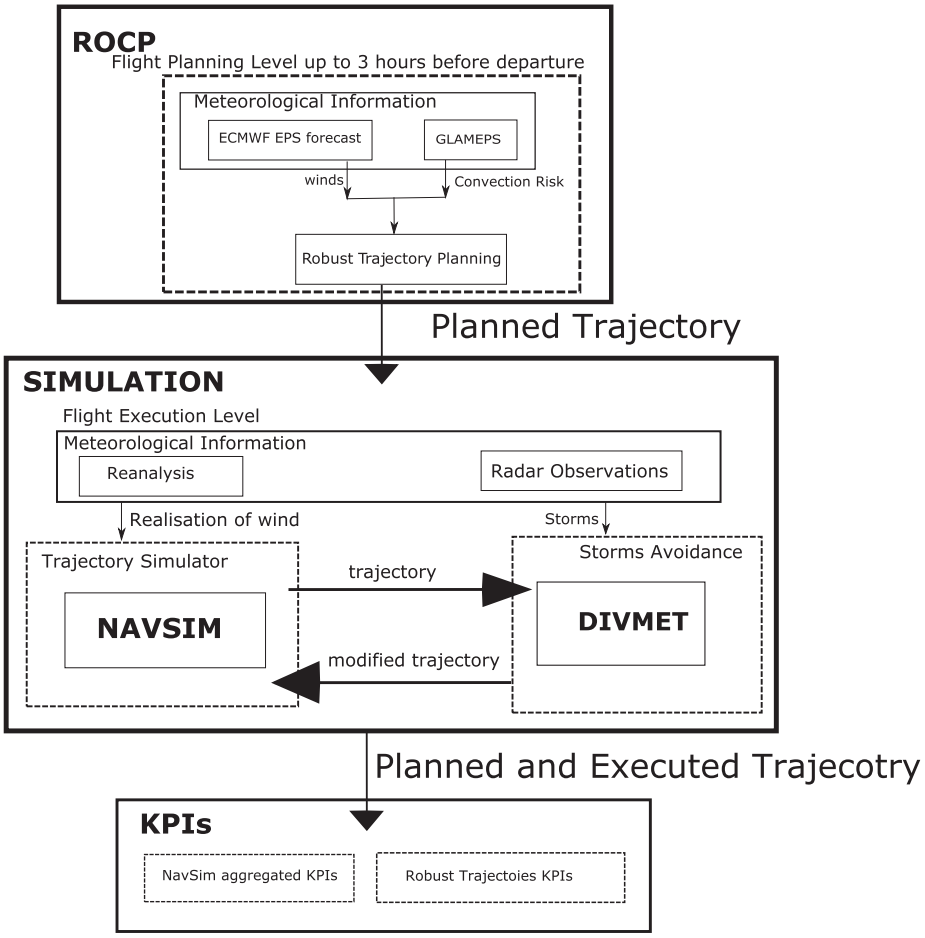

Fig. 1. Methodology.

with an estimated cost of 491 million € (EUROCONTROL, 2018).

Thunderstorms are particularly disruptive because of the complexity of predicting their formation and evolution at flight planning timescales (1–3 h before departure). Although particular (necessary but not sufficient) meteorological conditions are needed for thunderstorm development and can be predicted in advance, the exact location and timing of convective initiation triggers are more difficult to define. This concept is explained by very complex, highly energetic atmospheric dynamics and the typical sizes and life-spans of thunderstorms (small compared to medium-range Numerical Weather Prediction (NWP) models with spatiotemporal data resolution). As a result, both individual thunderstorm forecasting and its subsequent flight evasion maneuver occur at shorter time-scales, i.e., during the execution stage, say 10 min to 60 min before the encounter.

The trajectory planning problem around thunderstorms at such tactical timescales has been tackled within the literature through different approaches and algorithms. Some of them are geometric procedures (Erzberger et al., 2016; Taylor et al., 2018) is based on graph-search algorithms, e.g., Dijkstra's algorithm, A* or D*, with genetic-based multi-objective heuristics. Hauf et al. (2013) presents the software tool DIVMET (Lozano-Perez, 1981) is based on convex hull scanning and pathfinding (Liu and Hwang, 2014; Matsuno et al., 2015; Hentzen et al., 2018; González-Arribas et al., 2019), incorporate uncertainty in either dynamics or thunderstorm development into the problem. Seenivasan et al. (2020) uses nonlinear model predictive control based on hybrid optimal control with logical constraints in a disjunctive form in the presence of a multi-cell storm in development.

If one resorts to flight planning timescales, the work is certainly more limited. Recent attention has been put into analyzing meteorological hazards and their effects on flight planning. In (Gonzalez-Arribas et al., 2018), the flight planning problem under wind uncertainty using a robust optimal control methodology was studied. The same problem has been solved with two approaches: (Franco et al., 2018) presents a hierarchical flight planning algorithm (based on Dijkstra's algorithm combined with trajectory predictor based on a Probabilistic Transformation Method (Vazquez et al., 2017)); and (Legrand et al., 2018) solves the problem with an approach based on dynamic programming. These works are focused, however, on winds and its associated uncertainty. Kim et al. (2015), Kim et al. (2016) consider the effects of both winds and turbulence.

Nonetheless, convection indicators can also be incorporated into flight planning algorithms, as in (González-Arribas et al., 2019). The term "convective area or region" can be defined as an area of potentially developing thunderstorms. In other words, a convective

Fig. 2. Traffic obtained from NEST.

area features necessary, though not sufficient, conditions for the development of individual thunderstorms. The onset and the location of those individual thunderstorms are (for the time being) impossible to determine with enough precision at flight planning timescales. However, favorable characteristics and conditions can be forecasted in advance to configure those convective areas, which may have a persistence of up to 60 h. Aircraft must not necessarily avoid convective regions, but require higher weather-related situational awareness by pilots and controllers. Trajectories flying through a convective area can be potentially subject to track modifications, eventually increasing delays and flight times. The magnitude of the latter depends, among other factors, on the type of thunderstorms embedded in the convective area, the density of cells, their orientation, the size of the gaps separating the thunderstorms, and the time of onset.

The goal of the paper is, thus, to investigate this topic, i.e., we try to assess the following research questions: can the consideration of convection into flight planning optimization tools (as in (González-Arribas et al., 2019)) lead to reducing airborne thunderstorm encounter, thus enhancing safety? The following question arising is: at what cost?.

We herein claim the following three contributions: first, the generalization of the robust flight planning method (that considers uncertain wind and exposure to convection) presented in (González-Arribas et al., 2019) to a multi-aircraft, multi origin–destination case study. Second, the evaluation of the resulting robust trajectories under realized-weather (winds and thunderstorms), using the simulator environment NAVSIM (Rokitansky et al., 2007) (for flight tracking) enhanced with the DIVMET tool (Hauf et al., 2013) (for airborne thunderstorm detection and avoidance). Third, and last, the quantification of an expected impact (based on the scenario proposed) derived from a future application of robust flight planning algorithms considering convection in terms of safety and efficiency.

The methodology we have followed is sketched in Fig. 1: First, raw meteorological data is collected from Ensemble Prediction Systems (EPS), out of which wind uncertainty and probability of convection indicators can be elaborated. Second, the Robust Optimal Control Problem (ROCP) methodology (González-Arribas et al., 2019) is employed to obtain robust flight plans. Then, the latter (obtained as a solution to the ROCP and defined by a sequence of waypoints) is introduced into the simulator tool (NAVSIM) (Rokitansky et al., 2007), which *flies* the given route using wind information retrieved from reanalysis (considered as the possible realization of wind), and also considering thunderstorms based on radar observations. NAVSIM has implemented the functionality to avoid thunderstorms during the execution of the flight based on DIVMET. Finally, flight times, fuel burns, and its associated dispersions are analyzed. Different Key Performance Indicators (KPI) are defined to that end.

2. Traffic scenario definition

The scenario is composed of trajectories crossing areas of convective weather conditions, since we want to study the impact of using a robust flight planning methodology considering convection. Scenario information is obtained from EUROCONTROL's NEST software, and it corresponds to the last filed flight plans from the airlines (i.e., initial trajectories, according to NEST nomenclature). The demand of the en-route ATC sector LECBLVU is analyzed from 6:00 to 13:00 on 19 December 2016, because in the Spanish Mediterranean coast critical thunderstorm phenomena were found at that time. The resulting dataset is composed of 351 flights; NEST initial trajectories can be seen in Fig. 2.

Since the present research uses two different temporal horizons, the planning and the execution levels, two sets of trajectories are

considered. The first one corresponds to the *planned trajectories* computed using ROC methodology. The second one coincides with the simulated *executed trajectories* as the result of simulating the planned trajectory under current weather (wind and thunderstorms). In this section, both sets are described.

2.1. Robust trajectory planning

The trajectory planning task requires the following information:

- Coordinates of the departure and arrival airports: obtained from NEST.
- Departure time: obtained from NEST.
- Arrival time: obtained from NEST, used as a reference time.
- Pressure altitude of 200 hPa. (approximately 38600 ft.) for all aircraft and the whole flight.
- Airspeed: the average cruise Mach provided by Eurocontrol's Base of Aircraft Data (BADA) 3.13 (Nuic, 2010) for the aircraft model that performs the flight is considered for the whole flight (from origin to destination), ranging from 0.63 to 0.85.
- Convection risk and winds: obtained from GLAMEPS and ECMWF EPS forecasts, respectively. Refer to weather information definition in Section 3.

In order to incorporate the probability of convection in the trajectory planning process, we will apply the methodology presented in (González-Arribas et al., 2019) to find routes that minimize a weighted sum of average flight time (from all EPS forecast) and convection risk (weighted with the "convection penalty" parameter *CP*), as denoted in Eq. (3). We will here summarize the method for the sake of completeness.

The probability of convection is computed through the combination of two indicators: the Total Total Index (TT) and the Convective Precipitation (CP). TT is computed with the temperature gradient between 850 and 500 hPa and the moisture content between 850 and 500 hPa. CP is the precipitation coming from clouds formed by warmer air rising because it is less dense than its surrounding area. The probability of convection is computed as follows:

$$p_c = \frac{N_c}{N} \tag{1}$$

where N_c is the ensemble members in the EPS where the TT is above a threshold and CP is greater than 0; and N is the total number of ensemble members of the EPS.

In order to define the exposure to convection, let $\kappa(\phi, \lambda)$ be the smoothed and interpolated probability of convection, where ϕ is the latitude, λ the longitude.

The exposure to convection measured in equivalent distance[1] flown along the route (s) is then:

$$EC = \int_{s_0}^{s_f} \kappa\left(\phi\left(s\right), \lambda\left(s\right)\right) ds. \tag{2}$$

The cost functional to minimize is

$$J = \mathbb{E}\left[t_f\right] + CP \cdot EC \tag{3}$$

where t_f is the flight time.

The higher the CP value, the less exposure to convective risk, and thus the more predictable the trajectory. This exposure to convective risk areas reduction would be at the cost of additional flight time and fuel consumption. Refer to (González-Arribas et al., 2019) for more details.

2.2. Executed trajectory

The executed trajectories are generated by simulating the planned trajectories and the pilot's decisions when a thunderstorm is encountered. Therefore, the goal is to emulate a realistic storm avoidance manoeuvre, e.g., when the pilot detects in the weather radar that the aircraft is to overfly through a storm in the near term. DIVMET-Algorithm (Hauf et al., 2013) is to some extent realistic enough to mimic the mentioned pilots actions. It uses thunderstorm observations (readers are referred to Section 3 for further information) as 2D impenetrable polygons; then, if a thunderstorm is encountered, a deviation from the nominal path is computed.

DIVMET calculates the thunderstorm avoidance maneuver; this tool determines the initial and final avoidance maneuver points. Moreover, the standard curves that make the trajectory tangent to a convex hull of the thunderstorms polygons plus a 5 NM safety margin as can be seen in the example in Fig. 3.

[1] By equivalent distance, we mean the distance flown over a region with a probability of convection equal to one.

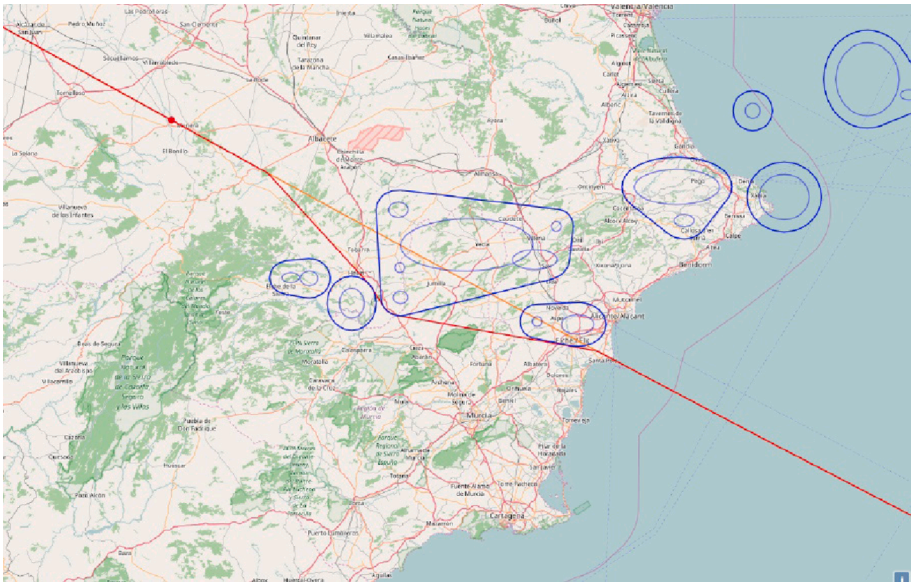

Fig. 3. Example of the deviation of thunderstorm cells by DIVMET. The red dot marks the aircraft position. The orange line shows the planned trajectory; the red line shows the thunderstorm avoidance maneuver. The thunderstorms cells (light blue) are surrounded by a safety margin of 5 NM resulting in a thunderstorm hull (dark blue). (For interpretation of the references to colour in this figure legend, the reader is referred to the web version of this article.)

3. Meteorological information

In the present paper, four meteorological products were used. Two of them are used in the flight planning level (up to 3 h before departure): ECMWF EPS and GLAMEPS. The other two meteorological products used in the flight execution level are Reanalysis and radar thunderstorms observations.

3.1. Ensemble prediction systems

Ensemble forecasting is a prediction technique that generates a representative sample of the possible future states of the atmosphere. An ensemble forecast is a collection of typically 10–50 weather forecasts (referred to as members) for the same forecast horizon, which can be obtained using different Numerical Weather Prediction (NWP) models with varying initial conditions. Each forecast may be based on a close, but a not identical model, to the best estimate of the model equations, thus representing the influence of model uncertainties on forecast error.

3.1.1. ECMWF

In this paper, we focus on the European Centre for Medium-Range Weather Forecasts (ECMWF) EPS for wind forecasts. Data can be accessed (among others) at the TIGGE dataset by the ECMWF.[2] (Park et al., 2008).

The ECMWF EPS is composed of 51 ensemble members (50 perturbed members and one control member) with approximately 32-km resolution up to forecast day 10 (65-km resolution after that), and 62 vertical levels.

EPS forecasts will provide ensemble-wise wind information to the ROCP method for trajectory planning. According to the flight plans retrieved from NEST, the earliest flight departs at 23:55 on 18 December. As a reference, the latest flight arrives at its destination at 17:15 on 19 December. The forecast area is defined considering the whole set of routes: from 24 degrees South to 61 degrees North, and from 96 degrees West to 56 degrees East, considering then an EPS area of −130 and 60 degrees in longitude and −45 and 75 in latitude. The spatial grid resolution is 0.25 degrees. The forecasts are retrieved for the pressure level 200 hPa, the selected barometric altitude for the flight. The ECMWF-EPS produces two forecasts at 00:00 and 12:00 each with time steps every 6 h. Therefore, the forecast used on each trajectory is determined (assuming static weather along the trajectory) in 2 steps:

- to select from both forecasts (at 00:00 or 12:00) the one released at least 3 h before departure (flight planning level),
- to select from all-time steps available the step that is close to the time at midway through the flight ($t_{Dep} + \frac{t_{Arr} - t_{Dep}}{2}$, where t_{Arr} and t_{Dep} are the arrival and departure times respectively both retrieved from NEST).

[2] http://apps.ecmwf.int/datasets/

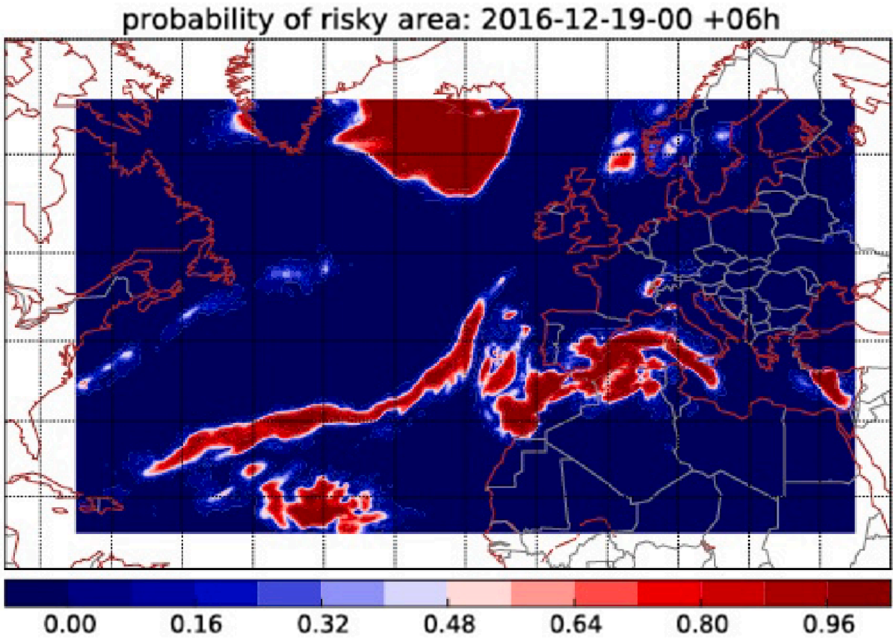

Fig. 4. Convective Risk map on 19/12/2016. Produced at 00.00 with time step 06.

3.1.2. GLAMEPS

The GLAMEPS ensemble with better resolution than ECMWF EPS of 12 km is a 48 + 4 member multi-model ensemble, with four control members plus 48 perturbed members, including a time-lag or lagging in half of the perturbed members. Time-lag is a special technique where predictions are made with several consecutive analysis over time, and it is often called Lagged Average Forecast (LAF) (AEMET, 2018). GLAMEPS is run over four cycles per day for hours 00, 06, 12, and 18 UTC, where each cycle runs a 24 + 4 member ensemble. The member configuration is such that two consecutive cycles make up a full 48 + 4 member ensemble. GLAMEPS comprises four models: Hirlam with Straco, Hirlam Karin/Fritsch, Alaro SURFEX, and Alaro ISBA.

A combination of two parameters was used to extract an indicator of convection: the Total Totals Index and the Convective Precipitation. The Total Totals Index can be post-processed by using temperature and dew point of different pressure levels provided as model output.

GLAMEPS forecasts will provide convective risk areas to the ROCP method. As for winds, convection is considered static along the trajectory, so the same procedure is done to compute the GLAMEPS forecast used on each trajectory. Fig. 4 illustrates the convective risk areas forecasted on 19/12/2016 (forecast produced at 00.00 with step 06 h). A high convective risk area over the Mediterranean Sea is observed. The GLAMEPS area used in this paper is −75 and 35 degrees in longitude and 15 and 65 in latitude.

3.2. ECMWF ERA-Interim Reanalysis

Reanalysis seeks to be the best estimate on winds and temperature variables. It is based on meteorological data assimilation. The aim is to assimilate historical observational data spanning an extended period, using a given model.

The ECMWF ERA-Interim Reanalysis will be used in the course of the validation activities. The data assimilation system used to produce ERA-Interim includes a 4-dimensional variational analysis (4D-Var) with a 12-h analysis window (Dee et al., 2011). The spatial resolution of the data set is approximately 80 km (T255 spectral) on 60 vertical levels from the surface up to 0.1 hPa. ERA-Interim products are typically updated once a month, with a delay of two months to allow for quality assurance and correct technical problems with the production. ERA-Interim data can be downloaded from the ECMWF Public Datasets. For detailed documentation of the ERA-Interim Archive, please refer to (Dee et al., 2011).

This reanalysis will provide wind values to the NAVSIM air traffic simulator. ECMWF ERA-Interim reanalysis produces two files at 00:00 and 12:00, so the selected one is close to the time at midway through the flight ($t_{Dep} + \frac{t_{Arr} - t_{Dep}}{2}$). The reanalysis area used is −130 and 60 degrees in longitude and −45 and 75 in latitude.

3.3. Thunderstorm radar observations

Observation data are derived from radar reflectivity and lighting data from the AEMET radar network covering then the Spanish territory, i.e., outlines of convective cells that delimit areas of high reflectivity (>37dBZ). It consists of convective cells that use mainly one level of radar data.

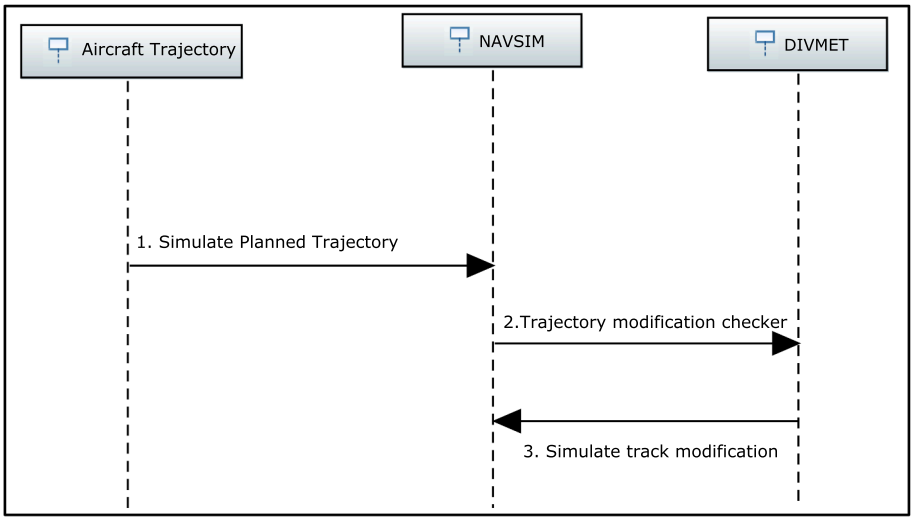

Fig. 5. Simulation sequence diagram scheme.

This weather product provides thunderstorm cells to the NAVSIM air traffic simulator and the DIVMET airborne thunderstorm detection and avoidance tool. The thunderstorm observations are updated every 10 min.

4. Simulation environment

Two tools, NAVSIM and DIVMET, were used to simulate the flight execution level, where the planned trajectories are flown, including weather observation (wind reanalysis and thunderstorms).

4.1. NAVSIM Infrastructure

NAVSIM is an ATM/ATC/CNS simulator developed by the University of Salzburg (Rokitansky et al., 2007). It is capable of simulating European air traffic based on specific reference days in the past (around 32.000 flights within 24 h), running as a real-time simulator, and a fast-time simulator. It allows accurate simulation, i.e., runway-to-runway or gate-to-gate.

NAVSIM is used to simulate the traffic scenario with the current wind weather fields (from the reanalysis). NAVSIM collects and processes information generated after the traffic scenario, such as total distance flown, total flight time, total fuel consumption, and the total number of track modifications from the nominal path.

4.2. DIVMET Infrastructure

DIVMET is a weather avoidance model tool that gives 2D guidance to provide meteorologically conflict-free aircraft trajectories, i.e., thunderstorms conflict-free routes. It simulates then the pilot decision when an adverse weather phenomenon is encountered, where those phenomena in real life are obtained typically throughout the on-board radar system and visual observation. It was initially developed by Hauf et al. (2013) and later applied experimentally in the terminal maneuvering area of Hong Kong International airport (Sauer et al., 2016).

DIVMET is used to compute the thunderstorms avoidance maneuver if the planned trajectory is conflicting with a thunderstorm cell. Once a thunderstorm free trajectory is obtained, this modified trajectory is sent to NAVSIM to be simulated.

5. Simulation procedure

Each trajectory from the traffic scenario defined in Section 2 was simulated. Five different runs (different CP parameters) were performed to analyze the convection risk influence in the optimal flight planning activity:

- CP = 0 s/m (minimum average flight time),
- CP = 0.005 s/m,
- CP = 0.010 s/m,
- CP = 0.015 s/m,
- CP = 0.020 s/m.

Recall that, in flight planning, the higher the CP value, the less exposure to convective risk. This reduction of exposure to convective

risk areas is, of course, at the cost of additional flight time and, thus, additional fuel consumption.

5.1. Planned trajectory simulation

The simulation task can be divided into four different activities, see Fig. 5. Each trajectory from the above-presented traffic scenario is introduced in NAVSIM to be simulated. The trajectories are introduced as a flight plan (sequence of Waypoints) to be flown under wind-extracted winds from the reanalysis weather product (realization of wind). The same aircraft dynamic and atmospheric model employed during the planning phase calculations are used to avoid adding simulation errors caused by other sources but weather uncertainties. To this end, three calibration tasks were developed before running the simulations:

- Kinematic calibration: one flight is simulated without wind. Then, flight times, distances, and speeds from the planning phase are compared with the one NAVSIM provides. This exercise identifies any possible inconsistency among others on Earth Model, Speeds, Altitudes, and Unity converters.
- Dynamic calibration: several flights are simulated (as many as aircraft types to be used) without any wind, and later fuel consumption is compared with NAVSIM results. This exercise is to identify any inconsistency on Aircraft model parameters (BADA), or fuel consumption models.
- Wind modeling error calibration: some flights are simulated with the deterministic wind (for instance, for each of the ensemble members). Then, flight time and fuel consumption discrepancies are compared with the one NAVSIM provides. This exercise is to identify any possible inconsistencies in wind modeling.

5.2. Trajectory modification checker

During the execution of the trajectory, NAVSIM passes trajectory information to DIVMET (latitude, longitude, altitude, time) to check if any thunderstorm is encountered. NAVSIM simulates the planned trajectory if it is not encountering any thunderstorm. Otherwise, in case of adverse weather, DIVMET computes the avoidance maneuver to navigate around the high-risk areas while at the same time keeping close to the original reference trajectory.

5.3. Track modification simulation

DIVMET thunderstorm avoidance maneuver is shared with NAVSIM to be simulated instead of the planned one that crossed a thunderstorm, as it is described in Section 2.2, an example of the DIVMET thunderstorm avoidance maneuver is shown in Fig. 3.

6. Key Performance Indicators (KPIs)

The following variables will be computed at both the flight planning and the execution level:

- Total number of track modifications from the nominal path (TF).
- Total distance flown (DF).
- Total flight time (FT).
- Total fuel consumption (FC).

Let us consider the following sets:

- $\mathcal{F} \rightarrow$ set of flights.
- $\mathcal{CP} \rightarrow$ set of CP values.
- $\mathcal{T} \rightarrow$ set of types of trajectories, i.e., flight planning (*RobustTrj*) or execution level (*NavSim*).Let us consider the following variables:

$$TF^k_{i,j}; \quad \forall i \in \mathcal{F}, \forall j \in \mathcal{CP}, \forall k \in \mathcal{T}.$$
$$DF^k_{i,j}; \quad \forall i \in \mathcal{F}, \forall j \in \mathcal{CP}, \forall k \in \mathcal{T}.$$
$$FT^k_{i,j}; \quad \forall i \in \mathcal{F}, \forall j \in \mathcal{CP}, \forall k \in \mathcal{T}.$$
$$FC^k_{i,j}; \quad \forall i \in \mathcal{F}, \forall j \in \mathcal{CP}, \forall k \in \mathcal{T}.$$

Thus, to compare the flight planning results with NAVSIM simulations, we must statistically characterize flight times and fuel consumption. The solution to the ROCP provides a planned trajectory that under EPS forecast winds gives a discrete number M (M equal to the number of members in the ensemble forecast) of possible values for both flight time and fuel consumption. Without loss of generality, mean values can be taken ($\forall i \in \mathcal{F}, \forall j \in \mathcal{CP}$):

$$Mean\left(FT_{i,j,m}^{\text{RobustTrj}}\right) \rightarrow \overline{FT_{i,j,m}^{\text{RobustTrj}}} = \sum_{m=1}^{M} \frac{FT_{i,j,m}^{\text{RobustTrj}}}{M}.$$

$$Mean\left(FC_{i,j,m}^{\text{RobustTrj}}\right) \rightarrow \overline{FC_{i,j,m}^{\text{RobustTrj}}} = \sum_{m=1}^{M} \frac{FC_{i,j,m}^{\text{RobustTrj}}}{M}.$$

The Key Validation Indicators to be evaluated are as follows:

$$\Delta TF_{i,j} = TF_{i,j}^{\text{NavSim}}; \forall i \in \mathcal{F}, \forall j \in \mathcal{CP}.$$

$$\Delta DF_{i,j} = \left\| DF_{i,j}^{\text{RobustTrj}} - DF_{i,j}^{\text{NavSim}} \right\|; \forall i \in \mathcal{F}, \forall j \in \mathcal{CP}.$$

$$\Delta FT_{i,j}^{\text{Mean}} = \left\| \overline{FT_{i,j}^{\text{RobustTrj}}} - FT_{i,j}^{\text{NavSim}} \right\|; \forall i \in \mathcal{F}, \forall j \in \mathcal{CP}.$$

$$\Delta FC_{i,j}^{\text{Mean}} = \left\| \overline{FC_{i,j}^{\text{RobustTrj}}} - FC_{i,j}^{\text{NavSim}} \right\|; \forall i \in \mathcal{F}, \forall j \in \mathcal{CP}.$$

Notice that in this case, in general, $DF_{i,j}^{\text{RobustTrj}} \neq DF_{i,j}^{\text{NavSim}}$, and thus $\Delta DF_{i,j} \neq 0$, will provide an indicator of deviations from the nominal path. Also, $TF_{i,j}^{\text{NavSim}} \neq 0$ (whereas $TF_{i,j}^{\text{RobustTrj}}$ is by definition zero since it acts as a nominal path). Also, $\|\cdot\|$ represents the absolute value of the difference.

Let us also define the following aggregated KPIs for the *RobustTrj* variables:

$$\Delta FT_j^{\text{Avg}} = \sum_{i \in \mathcal{F}} \frac{\Delta FT_{i,j}^{\text{Mean}}}{N_{flights}}; \quad \forall j \in \mathcal{CP}.$$

$$\Delta FC_j^{\text{Avg}} = \sum_{i \in \mathcal{F}} \frac{\Delta FC_{i,j}^{\text{Mean}}}{N_{flights}}; \quad \forall j \in \mathcal{CP}.$$

$$\Delta DF_j^{\text{Avg}} = \sum_{i \in \mathcal{F}} \frac{\Delta DF_{i,j}}{N_{flights}}; \quad \forall j \in \mathcal{CP}.$$

$$\Delta TF_j^{\text{Avg}} = \sum_{i \in \mathcal{F}} \frac{\Delta TF_{i,j}}{N_{flights}}; \quad \forall j \in \mathcal{CP}.$$

We would expect all of them $\Delta FT_j^{\text{Avg}}, \Delta FC_j^{\text{Avg}}, \Delta DF_j^{\text{Avg}}, \Delta TF_j^{\text{Avg}}$ to decrease as CP increases.

To find trade-offs between predictability (measured as ΔFT_j^{Avg} and $\Delta FC_j^{\text{Avg}}, \forall j \in \mathcal{CP}$) and efficiency, we will also compute average flight times and fuel consumption for the different CP values for the *NavSim* variables as follows:

$$TF_j^{\text{Avg}} = \sum_{i \in \mathcal{F}} \frac{TF_{i,j}^{NavSim}}{N_{flights}}; \quad \forall j \in \mathcal{CP}.$$

$$DF_j^{\text{Avg}} = \sum_{i \in \mathcal{F}} \frac{DF_{i,j}^{NavSim}}{N_{flights}}; \quad \forall j \in \mathcal{CP}.$$

$$FT_j^{\text{Avg}} = \sum_{i \in \mathcal{F}} \frac{FT_{i,j}^{\text{NavSim}}}{N_{flights}}; \quad \forall j \in \mathcal{CP}.$$

$$FC_j^{\text{Avg}} = \sum_{i \in \mathcal{F}} \frac{FC_{i,j}^{\text{NavSim}}}{N_{flights}}; \quad \forall j \in \mathcal{CP}.$$

7. Results

First, we present results in an aggregated manner in Section 7.1. Then, in Section 7.2, we focus on a single flight. Recall that results are presented and analyzed at two different levels. In first place, at the planning level, in which we use the ROCP methodology and provide the flight plan prediction or intention. In the planning level, weather information has been considered to be static (i.e., not evolving with time). In second place, at the execution level, the planned routes using NAVSIM-DIVMET incorporating wind and thunderstorm observations are simulated. In the latter, time-deviations due to winds and reroutings due to thunderstorm encounters are considered. Note that in this execution level, thunderstorm observations are only for the Spanish airspace. The results only show the effect in those segments in the trajectories that are in the Spanish airspace. An extension to wider areas would be needed for more

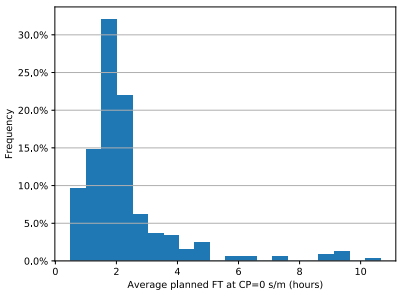

(a) Histogram at CP=0 s/m

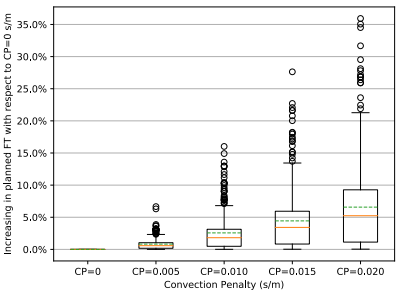

(b) Increasing in planned FT with respect to CP=0 s/m

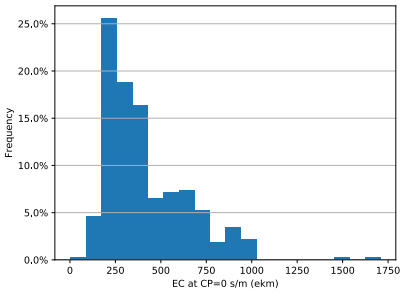

(c) Histogram EC at CP=0 s/m

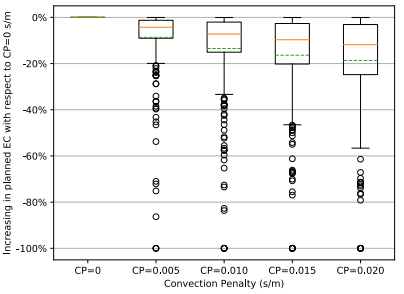

(d) Decreasing in planned EC with respect to CP=0 s/m

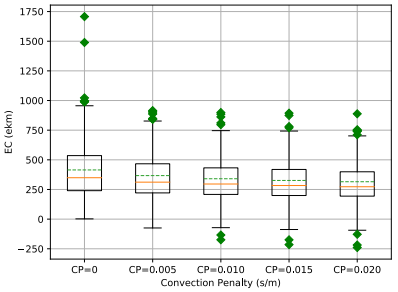

(e) Exposure to convection

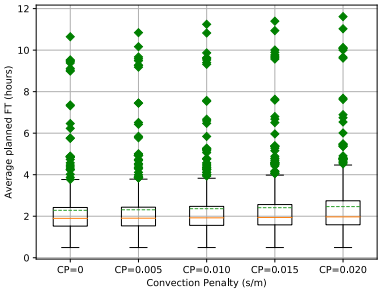

(f) Flight times

Fig. 6. Aggregated results.

Table 1
Quantitative values of exposure to convection (e-km), for different percentiles.

	Mean	P90	P75	P50	P25
CP = 0 s/m	414.9	736.5	539.2	349.1	239.9
CP = 0.005 s/m	365.8	674.4	466.5	310.4	220.4
CP = 0.010 s/m	340.2	632.1	431.8	294.8	208.2
CP = 0.015 s/m	326.6	615.1	417.0	278.5	198.4
CP = 0.020 s/m	316.6	600.3	397.5	270.8	193.8

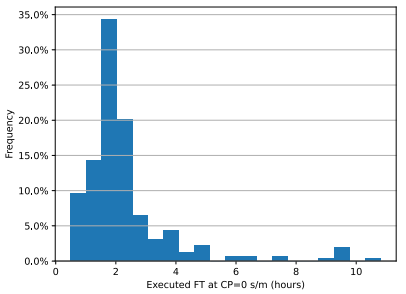

(a) Histogram for the executed flight times (FT) at CP=0 s/m

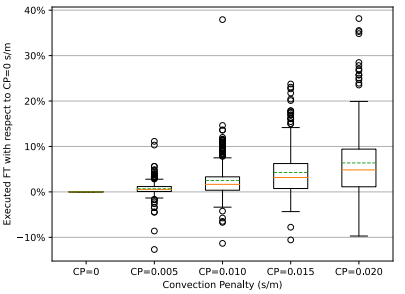

(b) Box plot for the relative variation in executed flight times (FT) w.r.t. convection penalty (CP)

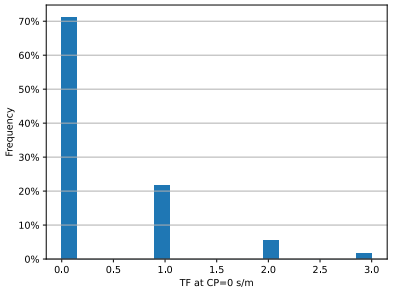

(c) Histogram for the track modifications (TF) at CP=0 s/m

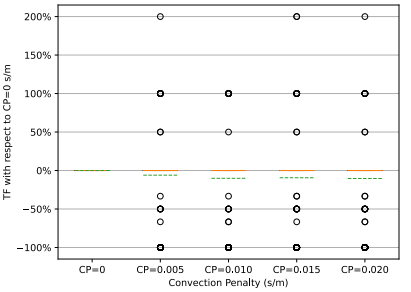

(d) Relative variation in track modifications (TF) w.r.t. CP=0 s/m

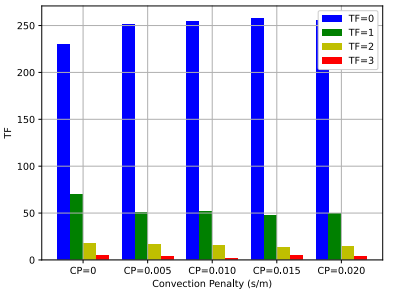

(e) Number of track modification (TF) w.r.t. the convection penalty (CP)

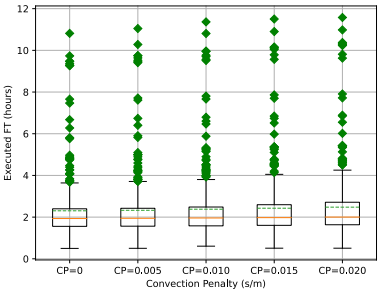

(f) Box plot for the absolute variation in executed flight times (FT) w.r.t. convection penalty (CP)

Fig. 8. Aggregated results at the executed level.

Table 2
Quantitative values of expected flight times (h), for different percentiles.

	Mean	P90	P75	P50	P25
CP = 0 s/m	2.28408333	3.75252778	2.42119444	1.89702778	1.52322222
CP = 0.005 s/m	2.31025	3.87375	2.43547222	1.90561111	1.53477778
CP = 0.010 s/m	2.36272222	4.11672222	2.47458333	1.92225	1.55955556
CP = 0.015 s/m	2.41119444	4.16744444	2.56183333	1.94058333	1.58369444
CP = 0.020 s/m	2.46347222	4.20833333	2.74383333	1.96883333	1.58788889

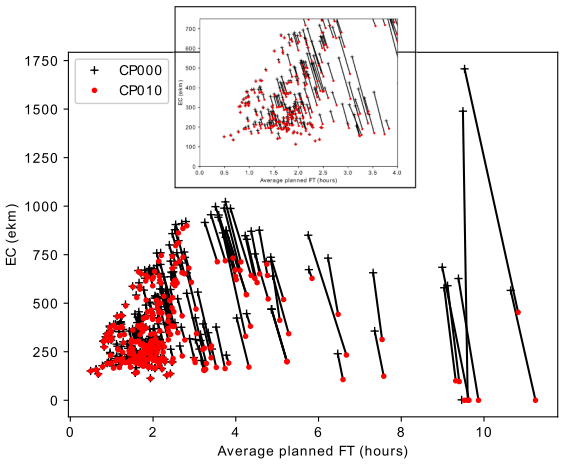

Fig. 7. Exposure to convection vs. Average planned Flight Time.

Table 3
Aggregated KPIs related to *TF*. The right-hand column refers to a number of km flown (as per aircraft) in an avoidance track due to thunderstorm encounter.

	TF_j^{Avg}	TF_j	# A/C with TF	km in avoidance track
CP = 0 s/m	0.375	121	93	74
CP = 0.005 s/m	0.301	97	72	44
CP = 0.010 s/m	0.273	88	69	34.9
CP = 0.015 s/m	0.273	88	65	33.4
CP = 0.020 s/m	0.279	90	68	30.4

Table 4
Aggregated KPIs related to FT, FC and DF, where ΔFT_j^{Avg} is in s, ΔFC_j^{Avg} is in kg, ΔDF_j^{Avg} is in m, FT_j^{Avg} is in s, FC_j^{Avg} is in kg, DF_j^{Avg} is in km. Refer to KPI definition in Section 6.

	ΔFT_j^{Avg}	ΔFC_j^{Avg}	ΔDF_j^{Avg}	FT_j^{Avg}	FC_j^{Avg}	DF_j^{Avg}
CP = 0 s/m	93.7	102.1	4258.0	8185	6181	1927
CP = 0.005 s/m	91.1	102.0	3250.9	8275	6256	1950
CP = 0.010 s/m	81.2	97.1	2731.8	8459	6397	1992
CP = 0.015 s/m	77.4	96.4	2309.0	8630	6516	2030
CP = 0.020 s/m	74.1	96.2	2440.5	8816	6639	2073

general claims, nevertheless the same behaviour is expected.

7.1. Aggregated results

7.1.1. Flight planning level

For all flights, and according to the routes provided by the ROCP methodology, the histogram in Fig. 6(a) and (c) shows the typology of our flights in the $CP = 0$ s/m where we observe that above 30% and 25% of the flights are 2 h on average and are exposed to 250*ekm*, respectively. In Fig. 6(e) we present exposure to convection values for different values of CP and in Fig. 6(d) the decreasing percentage to the value at $CP = 0$ s/m. Quantitative values can be consulted in Table 1. It can be readily seen that predicted exposure to convection systematically decreases as the CP parameter increases.

Nevertheless, such a reduction in exposure to convection comes at the cost of extra-expected flight time (and thus, associated extra fuel consumption). These values can be consulted in Fig. 8(f). In Fig. 6(b), the increasing percentage concerning the value at CP = 0 s/m is shown. Quantitative values can be seen in Table 2.

In Fig. 7, the relationship between EC and average FT in the planned flights is shown. In the area where the majority of the flights are located, as it was previously observed from Fig. 6(a) and (c), the CP = 0 s/m and CP = 0.010 s/m trajectories are very similars in terms of EC and average FT (the dot and the cross symbols are closer).

In aggregated terms, considering, for instance, P75 values (percentile 75), exposure to convection reduction (from CP = 0 to CP = 0.010 s/m) is slightly over 110 e-km at the cost of roughly 3 min of extra flight.

For the worst-case flight, a flight Punta Cana-Munich, the exposure to convection for the minimum expected time flight (CP = 0) is

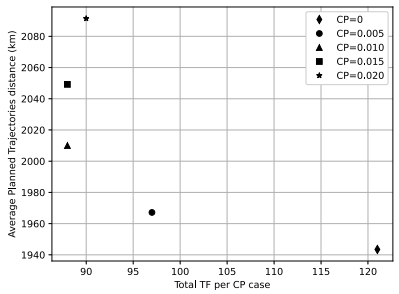

(a) Average trajectories distances and Total number of track modifications from the nominal path comparison per CP value.

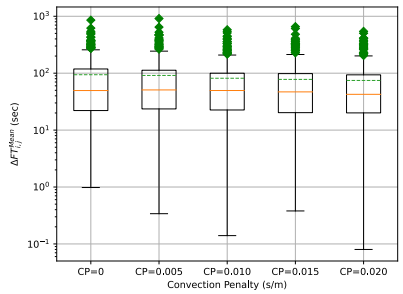

(b) Total flight time key validation indicator for every flight at every CP.

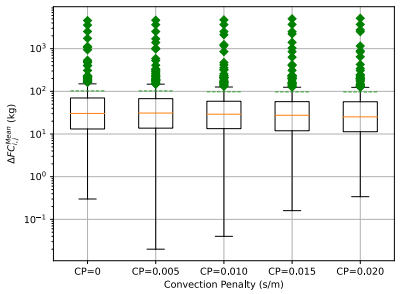

(c) Total fuel consumption key validation indicator for every flight at every CP.

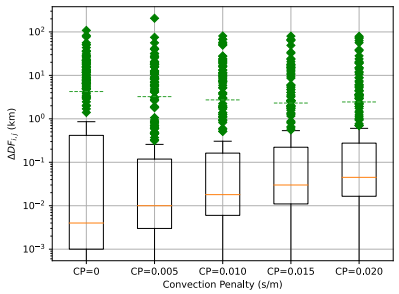

(d) Total distance flow key validation indicator for every flight at every CP.

Fig. 9. Aggregated KPIs related to *FT*, *FC* and *DF*.

around 1700 e-km. For CP's values different than zero, e.g., CP = 0.005 s/m, the exposure to convection decreases drastically, becoming close to zero.

7.1.2. Flight execution level

The categorization of the flights (looking at the executed level scenario for CP = 0 s/m) shows that roughly 35% of the flights have a duration of 2 h or less, see Fig. 8(a). In Fig. 8(b), the mean value of flight duration (denoted as green dash line in the figure) increases with CP value. Absolute flight durations as a function of CP are presented in Fig. 8(f). Note that, though the increase in flight duration as CP grows is the trend, there might be cases in which it goes the opposite. This is due to two main reasons: on the one hand, wind realizations (considered to be the reanalysis data in this experiments) differ from wind forecast; on the other, some track modification due to thunderstorm encounter might result in a short-cut, decreasing thus the total flight time.

We resort now to the analysis of track modifications. Results obtained executing the flight plans with NAVISIM-DIVMET simulation environment are presented in Tables 3 and 4. In Table 3, TF denotes the total number of advisories (due to thunderstorms) in each scenario (i.e., for different CP values). The column labeled "# A/C with TF" denotes the total number of aircraft affected by one (or more) advisories. The number of TF from the nominal path, see Fig. 8(c), shows that (for CP = 0 s/m) more than 20% of the flights need one track modification, 5% of the flights need two track modifications, and less than a 3% of the flights need three track modifications. It can be observed that the number of TF decreases as CP grows in mean values (green dash line in Fig. 8(d)). The absolute number of TF needed for different CP values is also presented in Fig. 8(e).

In quantitative terms analyzing only the executed trajectory, and comparing, for instance, CP = 0 and CP = 0.010 s/m scenarios (see Table 3 and 4). We observe how the number of advisories is reduced from 121 to 88, also reducing the aircraft affected from 93 to 69 (notice that a single aircraft might be affected by more than one advisory along the route), and the per-aircraft km flown in Cb avoidance maneuver from 74.2 to 34.9. This avoidance maneuver comes at the cost of extra flight time (275 s on average), extra fuel consumption (215 kg on average), and extra-distance flown (roughly 65 km on average).

7.1.3. Planning and execution level results

We analyse the indicators that compare both planned and executed trajectories, the same trends can be observed in Fig. 9(a), where lower CP values present lower planned flown distances with greater track modifications (TF) in the execution level. This means that lower CP will present shorter routes in the planning level, yet resulting in more track modification to avoid thunderstorms at the

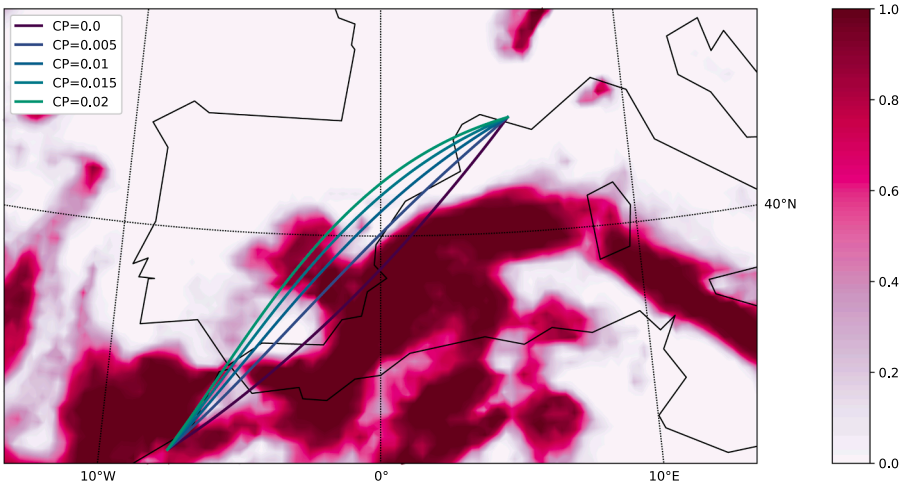

(a) Planned flights represented with the convective phenomena.

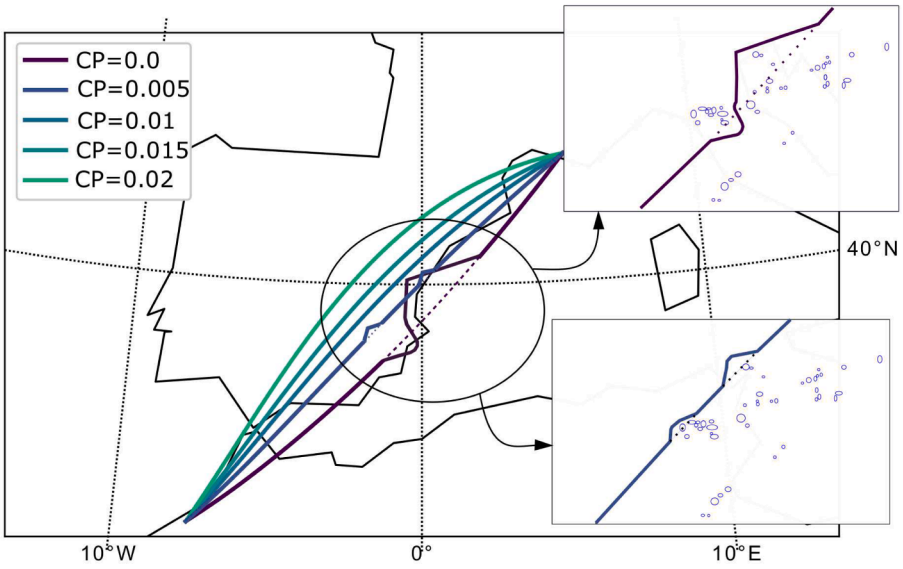

(b) Executed flights.

Fig. 10. Representative flight GMMN-LFML.

executing level. In particular, looking at CP = 0 s/m, 120 track modifications were observed for an average flight plan distance of 1940 km. Looking now at CP = 0.010 s/m values, the number of track modifications decrease bellow 90 for an average planned flown distance of nearly 2010 km. Also, it is shown that greater values than CP = 0.010 s/m do not provide a reduction in TF, however the flight plan average distance increases.

Moreover, it can be seen that the predictability is increased, since ΔFT_j^{Avg}, ΔFC_j^{Avg}, and ΔDF_j^{Avg} decrease as CP parameter increases, see Table 4 and Fig. 9(b), (c), (d). This behavior is, of course, due to the fact that the higher the CP, the lower the number of advisories and, thus, the less the deviations from the planned route.

In the ΔDF_j^{Avg} indicator there is a decreasing trend (as CP grows). Nevertheless, the behavior is not systematic (e.g., between CP = 0.015 s/m and CP = 0.020 s/m). The rationale is as follows: in some cases, when avoiding thuderstorms, the nominal track is a short-cut, and the distance is reduced.

7.2. Representative Flight (GMMN-LFML)

A flight GMMN-LFML (Casablanca Mohammed V Intl -Marseille Provence) is chosen to illustrate results further. Planned and executed flights for five different CPs can be seen in Fig. 10. In Fig. 10(a), we can see that planned trajectories are avoiding the

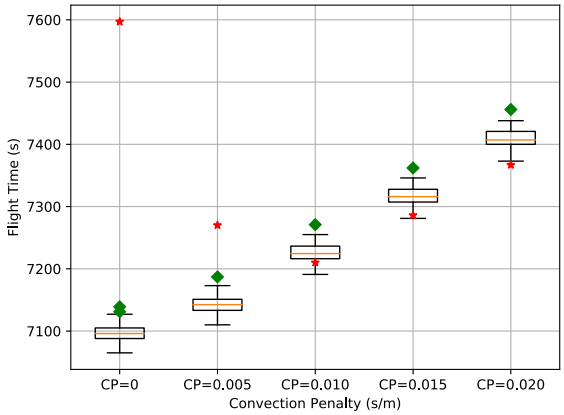

Fig. 11. Flight times GMMN-LFML.

Table 5
Executed flight GMMN-LFML.

	DF (km)	FT (s)	FC (kg)	TF
CP = 0 s/m	1692.15	7597	3521	1
CP = 0.005 s/m	1607.76	7270	3374	2
CP = 0.010 s/m	1588.31	7210	3347	0
CP = 0.015 s/m	1600.92	7286	3381	0
CP = 0.020 s/m	1615.53	7367	3418	0

convective areas over the Mediterranean sea. Meanwhile, in Fig. 10(b), we can observe that only thunderstorm phenomena affected CP = 0 and CP = 0.005 trajectories. A detailed insight in the CP = 0 and CP = 0.005 s/m thunderstorm maneuvering can be found in Fig. 10(b), where the blue lines are the thunderstorms, the solid lines are the flown trajectory, and the dotted lines are the planned trajectory.

Fig. 11 combines both the flight planning and flight execution results. The red-start denotes executed flight values (with observed winds and thunderstorms): recall that should a thunderstorm be encountered, the trajectory would deviate from the planned route. Conversely, the boxplot denotes values of the planned trajectory, which incorporate information of each of the 50 members that compose the ensemble forecast. In other words, the planned trajectory provides 50 possible flight times (and fuel consumption) for the same route-path. Quantitative values are given in Table 5.

If we look at the number of advisories, for flight plans computed with CP = 0 s/m, the execution results in one advisory, being two in CP = 0.005 s/m and zero with the other CP values. Indeed, the biggest executed flight time is that of CP = 0 s/m (the shortest at the planning level). The reason for that is because the wind-optimal trajectory (CP = 0 s/m) does not consider convection areas, thus planning to fly convective areas that might potentially develop into thunderstorms, as in this case, thus the need to deviate, see Fig. 10. On the contrary, in the CP = 0.010 s/m scenario, the planned trajectory is partially avoiding convective areas, see Fig. 10. Therefore, despite having planned for longer and more costly route, it turns to be the most efficient route after execution. It is not only that is not encountering any thunderstorm (with implications in terms of safety or complexity). It is also that it is not subject to deviations, being also more predictable. Note, indeed, that the execution fits *better* into the planned values in the three cases with no track deviations. The reader is referred to Table 5 for a quantitative insight.

8. Conclusion

This study validates a flight planning enhancement model, including forecasted convection and wind information. For this, a scenario of 351 trajectories was taken. Planned trajectories were optimized using different convection penalty parameters. A simulation to see the advantages of more predictable trajectories in terms of convection is performed, including wind and thunderstorm information taken from reanalysis and radar observations, respectively.

The robust optimal control problem methodology works properly when providing flight plans that are more predictable (by reducing exposure to areas of convection) at the cost of being (on average) more costly (in terms of flight time and fuel consumption). Other indirect savings of this increase in predictability (reduction in time-buffers, fuel reserves, holdings, or tactical ATFM regulations) have not been assessed and remain as future work. On average, and for this particular scenario, the trajectory becomes more predictable by increasing the CP parameter. Moreover, significant reductions of thunderstorm encounters (and thus thunderstorm avoidance maneuvers) have also been shown, which have a positive impact on safety and traffic complexity. In particular, a 25% reduction in thunderstorm avoidance maneuvering implies a 7.7% increase in flight time, on average.

Declaration of Competing Interest

None.

Acknowledgments

This work has been supported by TBO-MET project (https://tbomet-h2020.com/), which has received funding from the SESAR JU under grant agreement No 699294 under EU's Horizon 2020 research and innovation programme. Consortium members are UNIVERSIDAD DE SEVILLA(Coordinator), AEMET (Agencia Española de Meteorología), METEOSOLUTIONS GmbH, PARIS-LODRON-UNIVERSITAT SALZBURG, and UNIVERSIDAD CARLOS III DE MADRID.

References

AEMET, Física del caos en la predicción meteorológica, 2018. doi:10.31978/014-18-009-X.20.
Dee, D.P., Uppala, S., Simmons, A., Berrisford, P., Poli, P., Kobayashi, S., Andrae, U., Balmaseda, M., Balsamo, G., Bauer, P., et al., 2011. The era-interim reanalysis: Configuration and performance of the data assimilation system. Quart. J. Roy. Meteorol. Soc. 137 (656), 553–597. https://doi.org/10.1002/qj.828.
EUROCONTROL, Performance review report of the european air traffic management system in 2018 (June 2019).
Erzberger, H., Nikoleris, T., Paielli, R.A., Chu, Y.-C., 2016. Algorithms for control of arrival and departure traffic in terminal airspace. Proc. Inst. Mech. Eng., Part G: J. Aerosp. Eng. 230 (9), 1762–1779. https://doi.org/10.1177/0954410016629499.
Franco, A., Rivas, D., Valenzuela, A., 2018. Probabilistic aircraft trajectory prediction in cruise flight considering ensemble wind forecasts. Aerosp. Sci. Technol. 82–83, 350–362. https://doi.org/10.1016/j.ast.2018.09.020.
Gonzalez-Arribas, D., Soler, M., Sanjurjo-Rivo, M., 2018. Robust aircraft trajectory planning under wind uncertainty using optimal control. J. Guid., Control, Dynam. 41 (3), 673–688. https://doi.org/10.2514/1.G002928.
González-Arribas, D., Soler, M., Sanjurjo-Rivo, M., García-Heras, J., Sacher, D., Gelhardt, U., Lang, J., Hauf, T., Simarro, J., 2019. Robust optimal trajectory planning under uncertain winds and convective risk. In: Electronic Navigation Research Institute (Ed.), Air Traffic Management and Systems III, Springer Singapore, Singapore, 2019, pp. 82–103. doi:10.1007/978-981-13-7086-1_6.
González-Arribas, D., Soler, M., Sanjurjo Rivo, M., Kamgarpour, M., Simarro, J., 2019. Robust aircraft trajectory planning under uncertain convective environments with optimal control and rapidly developing thunderstorms. Aerosp. Sci. Technol., vol. 89. doi:10.1016/j.ast.2019.03.051.
Hauf, T., Sakiew, L., Sauer, M., 2013. Adverse weather diversion model divmet. J. Aerosp. Oper. 2, 115–133. https://doi.org/10.3233/AOP-130037.
Hentzen, D., Kamgarpour, M., Soler, M., González-Arribas, D., 2018. On maximizing safety in stochastic aircraft trajectory planning with uncertain thunderstorm development. Aerosp. Sci. Technol. 79, 543–553. https://doi.org/10.1016/j.ast.2018.06.006.
Kim, J.-H., Chan, W.N., Sridhar, B., Sharman, R.D., 2015. Combined winds and turbulence prediction system for automated air-traffic management applications. J. Appl. Meteorol. Climatol. 54 (4), 766–784. https://doi.org/10.1175/JAMC-D-14-0216.1.
Kim, J.-H., Chan, W.N., Sridhar, B., Sharman, R.D., Williams, P.D., Strahan, M., 2016. Impact of the north atlantic oscillation on transatlantic flight routes and clear-air turbulence. J. Appl. Meteorol. Climatol. 55 (3), 763–771. https://doi.org/10.1175/JAMC-D-15-0261.1.
Legrand, K., Puechmorel, S., Delahaye, D., Zhu, Y., 2018. Robust aircraft optimal trajectory in the presence of wind. IEEE Aerosp. Electron. Syst. Mag. 33 (11), 30–38. https://doi.org/10.1109/MAES.2018.170050.
Liu, W., Hwang, I., 2014. Probabilistic aircraft midair conflict resolution using stochastic optimal control. IEEE Trans. Intell. Transp. Syst. 15 (1), 37–46. https://doi.org/10.1109/TITS.2013.2274999.
Lozano-Perez, T., 1981. Automatic planning of manipulator transfer movements. IEEE Trans. Syst., Man, Cybernet. 11 (10), 681–698. https://doi.org/10.1109/TSMC.1981.4308589.
Matsuno, Y., Tsuchiya, T., Matayoshi, N., 2015. Near-optimal control for aircraft conflict resolution in the presence of uncertainty. J. Guidance, Control, Dynam. 39 (2), 326–338. https://doi.org/10.2514/1.G001227.
Nuic, A., 2010. User manual for the base of aircraft data (bada) rev 3.11, Atmosphere 2010 (2010) 001.
Park, Y.-Y., Buizza, R., Leutbecher, M., 2008. Tigge: Preliminary results on comparing and combining ensembles. Quart. J. Roy. Meteorol. Soc. 134 (637), 2029–2050. https://doi.org/10.1002/qj.334.
Rokitansky, C.-H., Ehammer, M., Gräupl, T., 2007. Newsky - building a simulation environment for an integrated aeronautical network architecture. In: 1st CEAS European Air and Space Conference, Berlin, Germany. CEAS, Brussels, Belgium, 2007, pp. 611–618. doi:10.1109/DASC.2007.4391905.
Sauer, M., Hauf, T., Sakiew, L., Chan, P., Tse, S.-M., Hupe, P., 2016. On the identification of weather avoidance routes in the terminal maneuvering area of hong kong international airport. J. Zhejiang Univ. Sci. A 17, 171–185. https://doi.org/10.1631/jzus.A1500186.
Seenivasan, D.B., Olivares, A., Staffetti, E., 2020. Multi-aircraft optimal 4d online trajectory planning in the presence of a multi-cell storm in development. Transport. Res. Part C: Emerg. Technol. 110, 123–142. https://doi.org/10.1016/j.trc.2019.11.014.
Taylor, C., Liu, S., Wanke, C., Stewart, T., 2018. Generating diverse reroutes for tactical constraint avoidance. J. Air Transport. 26 (2), 49–59. https://doi.org/10.2514/1.D0089.
Vazquez, R., Rivas, D., Franco, A., 2017. Stochastic analysis of fuel consumption in aircraft cruise subject to along-track wind uncertainty. Aerosp. Sci. Technol. 66, 304–314. https://doi.org/10.1016/j.ast.2017.03.027.